

## Stability and band offsets of polar GaN/SiC(001) and AlN/SiC(001) interfaces

M. Städele, J. A. Majewski, and P. Vogl

*Physics Department and Walter Schottky Institute, Technical University Munich, Am Coulombwall, D-85748 Garching, Germany*

(Received 5 February 1997)

We present first-principles calculations of structural and electronic properties of polar [001]-oriented interfaces between  $\beta$ -SiC substrates and strained cubic GaN or AlN. The formation enthalpies of reconstructed interfaces with one and two mixed layers and lateral  $c(2\times 2)$ ,  $2\times 1$ ,  $1\times 2$ , and  $2\times 2$  arrangements are calculated. We find interfaces containing C-N “donor” and Si-Ga “acceptor” bonds to be energetically highly unfavorable. The most stable interfaces are predicted to possess unsaturated Ga-C and Si-N bonds only. Simple electrostatic arguments suffice to explain the energetically lowest lateral reconstructions among structures that have the same chemical composition. The present self-consistent total-energy minimizations show that atomic relaxations play a crucial role both energetically as well as for the band offsets. Qualitatively, these relaxations can be understood as size effects of the constituent atoms. The electronic valence-band offsets of various stoichiometric interface structures of GaN/SiC(001) and AlN/SiC(001) heterojunctions are found to depend strongly on the chemical composition of the interface layers but are less sensitive to the type of lateral reconstruction. Interfaces that have different chemical compositions but comparable formation enthalpies lead to valence-band offsets in the ranges of 0.8–1.8 eV and 1.5–2.4 eV, respectively, depending on the detailed interface mixing. However, the valence-band maximum is found to lie higher in SiC than in GaN or AlN in all cases. [S0163-1829(97)09236-9]

### I. INTRODUCTION

The III-V nitrides GaN, AlN, and their alloys appear to be promising candidates for high-power, high-temperature, and high-frequency microelectronic applications as well as for blue and ultraviolet light-emitting diodes and lasers.<sup>1–4</sup> So far, most of the research has focused on GaN, but AlN-based heterosystems<sup>5–9</sup> show some advantages due to the larger band gap of 6.2 eV and the excellent thermal and chemical characteristics of AlN.<sup>10</sup>

A major challenge for applications is the lack of a suitable lattice-matched substrate that allows pseudomorphic and defect-free heteroepitaxial growth of GaN. The most commonly used substrate is sapphire ( $\text{Al}_2\text{O}_3$ ) even though it shows a huge 14% (12%) lattice mismatch relative to GaN (AlN). A range of alternatives such as Si, GaAs, InP, ZnO, MgO, and  $\text{Mg}_2\text{Al}_2\text{O}_4$  has been looked at,<sup>1,10,11</sup> but the resulting films still suffer from very high defect densities of the order of  $10^{10} \text{ cm}^{-2}$ , which limits the lifetime of electronic devices considerably. SiC seems to be one of the most promising substrate materials at the present time since there is a relatively low lattice mismatch between SiC and GaN ( $\approx 3.5\%$ ), and especially AlN ( $\approx 0.5\%$ ). In addition, SiC and the nitrides exhibit very similar thermal expansion characteristics and possess the same types of structural modifications, namely, cubic zinc blende and hexagonal wurtzite structures. Epitaxial growth has been studied both on the cubic  $3C$  phase  $\beta$ -SiC (Refs. 12–17) and the hexagonal  $6H$ -SiC.<sup>18–22</sup> Whereas the wurtzite structure is the equilibrium bulk phase of the nitrides, their zinc blende phase is of considerable interest as well. It forms during growth onto the (001) surface of cubic SiC substrates<sup>12–17</sup> and is expected to have superior electrical properties.<sup>2,10</sup>

In this paper, we present *ab initio* local-density-functional calculations of formation enthalpies and band discontinuities

of polar interfaces between cubic SiC(001) substrate and lattice-matched, strained zinc blende GaN or AlN. Since abrupt polar interfaces are energetically unstable with respect to the interdiffusion of atoms across the interface,<sup>23,24</sup> we consider several intermixed, reconstructed, and fully relaxed geometries and compare their relative stability. Electronic and ionic degrees of freedom are fully taken into account. Indeed, the atomic relaxation near the GaN/SiC interface is significant due to the 3.5% mismatch between the bulk lattice constants of SiC and GaN. Thus, this relaxation greatly affects electronic properties such as band offsets.

Most theoretical investigations have focused on the cohesive and electronic properties of bulk nitrides up to now,<sup>25–36</sup> whereas fewer publications have dealt with nitride heterostructures. Electronic structure calculations have been performed for short-period GaN/AlN superlattices in the wurtzite<sup>37,38</sup> as well as in the zinc blende<sup>37,39</sup> structure. In addition, valence-band offsets have been predicted for pseudomorphic GaN/AlN, GaN/InN, and AlN/InN zinc blende<sup>36,39</sup> and wurtzite<sup>36</sup> heterostructures. Little is yet known, however, about the detailed microscopic atomic structure of nitride-substrate interfaces such as GaN/SiC and AlN/SiC and the corresponding band discontinuities. Semiempirical tight-binding calculations have predicted formation energies for various nonpolar AlN/SiC interfaces,<sup>40</sup> unreconstructed hexagonal GaN/SiC(0001) interfaces,<sup>41</sup> and for reconstructed polar GaN/SiC(001) interfaces.<sup>42</sup> The latter paper focused on reconstructed  $\beta$ -SiC surfaces with a GaN coverage of a few monolayers. The only first-principles studies we are aware of have studied the stability and band offsets of the nonpolar AlN/SiC zinc blende [110] interface,<sup>43</sup> and total energies of [0001]-oriented GaN (Ref. 44) and AlN (Ref. 45) films on a hexagonal SiC substrate.

A characteristic of SiC and nitride heterostructures is the significant amount of strain that adds to the complications

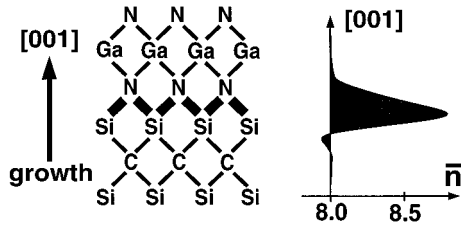


FIG. 1. Schematic view and averaged valence electron density  $\bar{n}$  perpendicular to the interface in an abrupt GaN/SiC(001) interface with Si-N donor bonds (marked by thicker lines).  $\bar{n}$  is normalized to the number of electrons in the bulk unit cell.

brought about by the polar nature of the interfaces. In most of the semiconductor heterostructure interfaces that were studied theoretically so far, strain played a negligible role, e.g., in Ge/GaAs,<sup>46–51</sup> ZnSe/GaAs,<sup>47,48,52</sup> ZnSe/Ge,<sup>47,48</sup> and Si/GaP (Ref. 51) heterostructures. A noticeable exception are the strained and reconstructed polar Si/GaAs interfaces that have been analyzed by *ab initio* studies in Refs. 51 and 53.

This paper is organized as follows. In Sec. II, we discuss the types of reconstructed interfaces that we have studied, and briefly define the basic quantities of interest, namely, formation enthalpies and band offsets. In Sec. III, we describe the computational schemes employed and give some numerical details. The main results and predictions are presented and discussed both quantitatively as well as qualitatively in Sec. IV. Section V gives a brief summary.

## II. CHARACTERISTICS OF RECONSTRUCTED INTERFACES

### A. Interface types with a single mixed layer

Abrupt, pseudomorphic [001] interfaces between cubic SiC and GaN (AlN) consist of two adjacent monoatomic layers. At such an abrupt interface, every chemical tetrahedral bond is a nonsaturated (or “wrong”<sup>54</sup>) bond with either more (termed “donor bond”) or less (termed “acceptor bond”) than two electrons, creating a macroscopically charged donor or acceptor interface. This is illustrated in Fig. 1, which depicts schematically an abrupt Si-N donor interface with a localized pileup of the electronic charge. This and the following figures also show electronic valence densities  $\bar{n}$  that are macroscopically averaged according to Eq. (7) and are results of the present *ab initio* calculations that will be discussed in detail in the subsequent sections. Naturally, such a highly charged interface is energetically unstable<sup>23,24,47,48,51,52</sup> and reconstructs in such a manner as to become neutral on the average, i.e., to contain as many donor as acceptor bonds. The simplest way to achieve this type of charge compensation in a donor (acceptor) interface is to replace every other group V (group III) atom by a group IV atom or, equivalently, every other group IV atom by a group III (group V) atom at the interface. The resulting interfaces contain an atomic layer with two chemical constituents that is sandwiched in between two monoatomic layers, as depicted schematically in Figs. 2(a) and 2(b). These figures also show that the electronic charge distribution near this interface is significantly smoother and more delocalized than in the abrupt case.

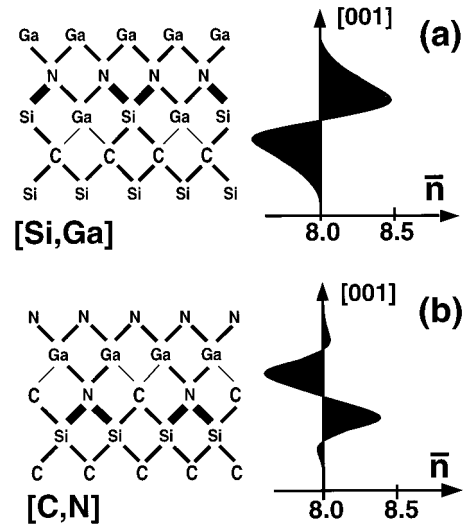


FIG. 2. Schematic views and averaged valence electron densities  $\bar{n}$  of the reconstructed GaN/SiC(001) interfaces with (a) one mixed [Si,Ga] and (b) one mixed [C,N] layer. Thicker and thinner lines mark donor and acceptor bonds, respectively.  $\bar{n}$  is normalized to the number of electrons in the bulk unit cell.

Interfaces with several mixed atomic layers have even smaller dipole moments and are able to distribute the donor and acceptor bonds more evenly across several layers, which can be energetically more favorable. In this paper, we have studied interface reconstructions both with one as well as with two mixed atomic layers. Indeed, experimental evidence for 6H-AlN/SiC interface reconstructions with only one mixed layer was presented recently by Ponce *et al.*<sup>55–57</sup> Similar types of reconstructions were also found in early stages of GaN growth on SiC (Ref. 58) and GaAs (Ref. 59) substrates.

Henceforth, we will focus on pseudomorphic [001]-oriented, intermixed, and reconstructed interfaces between zinc blende SiC substrate and (strained) zinc blende GaN. The most general atomic layer sequence perpendicular to such an interface with a *single* mixed interface layer can be written in the form (the mixed layer is indicated by brackets)

$$\dots c-s-c-[s_{x_s}c_{x_c}g_{x_g}n_{x_n}]-n-g-n\dots \quad (1)$$

Here, the atomic layers parallel to the (001) plane have been denoted by lowercase letters in order to be able to discuss all possible interface combinations together. Adjacent atomic layers denoted by *c-s* represent *either* the sequence C-Si or Si-C. Similarly, the adjacent layers *n-g* stand for *either* N-Ga or Ga-N. Note that the atomic layers next to the mixed interface layer are *c* on one side (i.e., C or Si) and *n* (i.e., N or Ga) on the opposite side, respectively.

In general, a compensated interface with one mixed layer may contain all four types of atoms Si, C, Ga, and N with corresponding concentrations  $x_{\text{Si}}$ ,  $x_{\text{C}}$ ,  $x_{\text{Ga}}$ , and  $x_{\text{N}}$  that obey the condition  $x_{\text{Si}} + x_{\text{C}} + x_{\text{Ga}} + x_{\text{N}} = 1$ . Many of these combinations are energetically unfavorable and physically implausible, however. Highly unsaturated or oversaturated III-III or V-V bonds are unlikely to form, as has already been pointed out previously for alloy systems.<sup>60,61</sup> Therefore, we exclude Ga-Ga or N-N bonds and require  $x_n = 0$ . Similarly, we re-

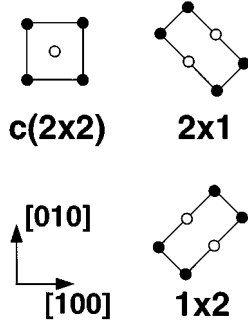
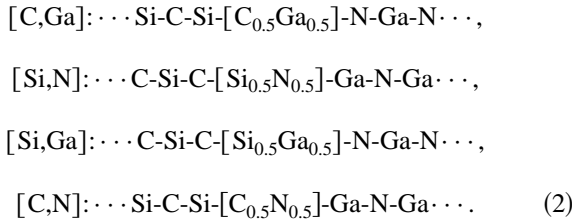


FIG. 3. Positions of the atoms in the single mixed (001) interface layer for  $c(2 \times 2)$ ,  $2 \times 1$ , and  $1 \times 2$  lateral reconstructions.

quire  $x_c = 0$ , thereby excluding all pure cation-cation (Si-Si) and anion-anion (C-C) bonds. The remaining  $s-n$  and  $c-g$  nonsaturated bonds act as donor and acceptor (or acceptor and donor) and must occur in pairs in order to guarantee charge compensation, which leads to the condition  $x_s = x_g = 0.5$ . In total, this gives four possible types of interfaces that can be labeled by the two types of atoms in the interface layer as follows:



Note that none of these  $[s,g]$  interfaces contains nonsaturated  $s-g$  bonds. Instead, there are 50% saturated bulk bonds, 25% nonsaturated  $c-g$  and 25% nonsaturated  $s-n$  bonds. Schematic views of the  $[\text{Si,Ga}]$  and  $[\text{C,N}]$  interfaces are depicted in Figs. 2(a) and 2(b).

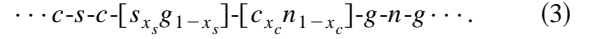
In the construction of each  $[s,g]$  interface, one additional degree of freedom remains, namely, the pattern formed by the atoms within the mixed layer. We have studied theoretically three different arrangements (shown in Fig. 3) that are compatible with charge compensation: a  $c(2 \times 2)$  reconstruction, where every atom of one type is surrounded by four atoms of the other type, and  $2 \times 1$  and  $1 \times 2$  reconstructions, where every atom has two like and two unlike neighbors. These types of reconstructions are not the only conceivable ones but they are the simplest and most common structures. In fact, recently similar types of reconstructions have been identified experimentally at SiC (Ref. 62) and GaN (Refs. 58 and 59) surfaces and for AlN/SiC (Ref. 56) and GaAs/Ge (Ref. 63) interfaces.

The laterally averaged valence electron densities parallel to the interface plane are, to an excellent degree of approximation, independent of the lateral reconstruction. Therefore, it is unnecessary to specify the type of lateral reconstruction in the previous Figs. 2(a) and 2(b).

### B. Interface types with two mixed layers

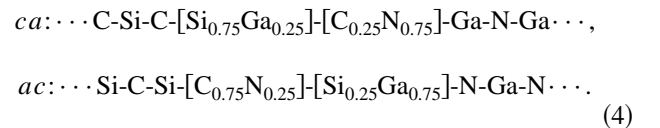
The number of possibilities to form interfaces with *two* adjacent mixed atomic layers is obviously even larger than for the previously discussed case. However, following the

same arguments as before, we restrict our focus on interfaces where (i) each of the two mixed layers contains exactly two kinds of atoms and (ii) there are no common atoms in any two adjacent layers. Using the same shorthand notation as before  $[(c,s) = (\text{C,Si}) \text{ or } (\text{Si,C})]$ ,  $(n,g) = (\text{N,Ga}) \text{ or } (\text{Ga,N})]$ , these conditions lead to the following sequence of atomic layers:



Charge compensation requires the number of  $s-n$  nonsaturated bonds to equal the number of  $c-g$  nonsaturated bonds. The  $s-n$  bonds occur only in between the two mixed layers and therefore have a concentration of  $x_s(1-x_c)$ . On the other hand, the  $c-g$  bonds occur not only between the two mixed layers with a concentration of  $x_c(1-x_s)$ , but also in between each mixed interface layer and its adjacent bulk layer with concentration  $1-x_s$  and  $x_c$ , respectively. By setting the sum of these concentrations equal to the concentration of the  $s-n$  bonds, one is finally led to the condition  $x_s - x_c = 0.5$  for a charge compensated interface.

This condition puts a constraint on the structure of the lateral unit cell. Let  $N_i$  be the number of atoms of species  $i$  and  $N_L$  the total number of atoms in the lateral unit cell. Since  $x_i = N_i/N_L$ , charge compensation requires  $N_L/2 = N_s - N_c$ . The smallest natural numbers that fulfill this relation are  $N_L = 4$ ,  $N_s = 3$ , and  $N_c = 1$ , which implies a concentration ratio of 3:1 for the two types of atoms in each of the two mixed layers. There are four such arrangements possible, that we label by  $ca$ ,  $ac$ ,  $ca'$ , and  $ac'$ , respectively. The structure  $ca$  contains cation-type atoms (Si and Ga) in the first layer and anion-type atoms in the second while the situation is reversed for the second structure  $ac$ . The structures are given by



The remaining two sequences  $ca'$  and  $ac'$  are obtained by swapping the atoms  $\text{Si} \leftrightarrow \text{C}$ . A schematic side view of the layer sequences, Eq. (4), and their average electron densities is shown in Fig. 4. We note that the total charge distributions across any of these interfaces possess a small but nonvanishing dipole moment as can be seen from the slight asymmetry in  $\bar{n}(z)$  in this figure. The magnitude of this dipole moment turns out to be almost the same for  $ca$  and  $ac$ .

We have not yet completely specified the arrangement of the atoms within the lateral unit cell. With  $N_L = 4$ , it may be arranged in a  $2 \times 2$  or a  $4 \times 1$  reconstruction pattern. In the subsequent section, we will show that there are very good reasons to expect homogeneous and isotropic types of charge arrangements with small unit cells to be energetically favorable. Therefore, we have only studied unit cells with four atoms per layer and  $2 \times 2$ -type reconstructions. Symmetry allows two types of  $2 \times 2$  arrangements, one containing four [termed  $2 \times 2(4)$ ] and the second one containing five [termed  $2 \times 2(5)$ ] donor and acceptor bonds per lateral unit cell. These two types of structures are depicted in Fig. 5. Since the laterally averaged valence electron densities are virtually

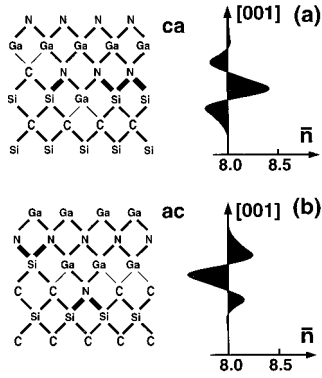


FIG. 4. Schematic views and averaged valence electron density  $\bar{n}$  of the (a)  $ca$  and (b)  $ac$  GaN/SiC interface with two mixed layers. Thicker and thinner lines mark donor and acceptor bonds, respectively.  $\bar{n}$  is normalized to the number of electrons in the bulk unit cell.

identical for the  $2 \times 2(4)$  and  $2 \times 2(5)$  reconstructions, Fig. 4 displays only the former situation.

In this paper, we focus on *pseudomorphically* grown GaN films on an unstrained SiC substrate. Consequently, the nitride films are biaxially strained with a lateral strain tensor element given by  $a_{\text{GaN}}/a_{\parallel}-1$ , and the lateral lattice constant  $a_{\parallel}=a_{\text{SiC}}$  equals the bulk lattice constant of  $\beta$ -SiC. In our calculations, we have modeled all heterostructures by stoichiometric superlattices containing an integer number of SiC and nitride bulk units, respectively. In this way, the physical quantities of interest, such as formation enthalpies and valence-band offsets (VBO) can be determined straightforwardly.

### C. Formation enthalpies and valence-band offsets

The relative stability of  $p \times q$  reconstructed interfaces can be assessed by computing the formation enthalpies  $\delta H_{\text{int}}$  of corresponding superlattices at zero temperature,

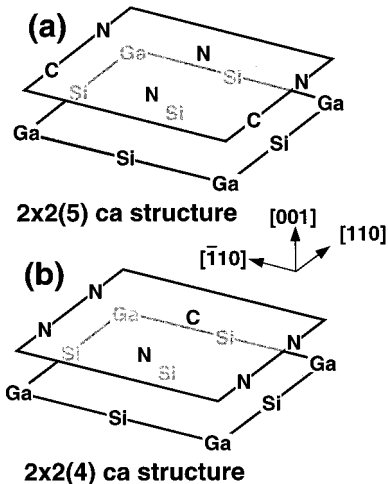


FIG. 5. Schematic view of lateral arrangements of atoms in the two mixed layers at the reconstructed (a)  $2 \times 2(5)$  and (b)  $2 \times 2(4)$   $ca$  interfaces of GaN/SiC(001).

$$\delta H_{\text{int}} = \frac{1}{2pq} (E_{\text{tot}}^{\text{sup}} - m_{\text{GaN}} E_{\text{tot}}^{\text{GaN}}[a_{\parallel}] - n_{\text{SiC}} E_{\text{tot}}^{\text{SiC}}[a_{\parallel}]). \quad (5)$$

Here,  $E_{\text{tot}}^{\text{sup}} = E_{\text{tot}}^{\text{sup}}(a_{\parallel})$  is the ground-state energy of the supercell with  $m_{\text{GaN}}$  and  $n_{\text{SiC}}$  chemical units of GaN and SiC, respectively. The total energy of this supercell is minimized with respect to all electronic and ionic degrees of freedom, with the only constraint of the lateral lattice constant being held fixed at  $a_{\parallel}$ . Apart from this constraint, all atomic positions in the unit cell as well as the lattice constant of the supercell in the growth direction are optimized. As indicated by the factor  $1/2$  in Eq. (5), this expression actually refers to the *average* formation enthalpy of both interfaces in the supercell. However, for [001] reconstructed interfaces that are of interest in this work, one can always find supercells where both interfaces are identical. In the case of the  $2 \times 1$  and  $1 \times 2$  reconstructions, this requires an enlargement of the lateral area of the supercell by a factor of 2.

The valence-band offset  $\Delta E_V$  at an interface between two semiconductors can be conveniently split up into two terms<sup>64</sup>

$$\Delta E_V = \Delta \bar{V} + \Delta E_{BS}, \quad (6)$$

where  $\Delta \bar{V}$  is the asymptotic difference between the laterally and vertically averaged electrostatic (Hartree plus ionic) potential  $V(\mathbf{r})$  in the superlattice far from the interface. This average  $\bar{V}(z)$  of the electrostatic potential at distance  $z$  from the interface can be defined by

$$\bar{V}(z) = \frac{1}{A_{\text{cell}}} \int dx dy \int dz' dz'' w_{\text{GaN}}(z-z') w_{\text{SiC}}(z'-z'') \times V(x, y, z''),$$

$$w_{\text{bulk}}(z) = \frac{1}{2d_{\text{bulk}}} \Theta(d_{\text{bulk}} - |z|). \quad (7)$$

Here,  $A_{\text{cell}}$  is the lateral unit cell area in the  $x, y$  plane,  $\Theta$  denotes the unit step function, and  $d_{\text{bulk}}$  is the [001] distance between atomic layers within the (strained) bulk materials (GaN, SiC) far from the interface. We have used an expression analogous to Eq. (7) for the macroscopically averaged electron density  $\bar{n}(z)$  in Figs. 1, 2, and 4. We note that the present results do not depend sensitively on the detailed choice of the weighting function  $w_{\text{bulk}}$  that averages out all short-range contributions to the potential. By integrating the Poisson equation across the interface and noting that the macroscopic electric field is zero deep inside the bulk materials, it follows that  $\Delta \bar{V}$  equals  $4\pi ep$ , where  $p$  is the dipole moment (per unit area) of the macroscopically averaged electronic *and* ionic charge density across the interface. It is nonzero due to the rearrangement of charge near the interface relative to the two bulk crystals and thus depends on the detailed interface geometry.

The second term in Eq. (6),  $\Delta E_{BS} = E_v(\text{SiC}) - E_v(\text{GaN})$ , is the difference between the eigenvalues of the top of the valence band in the two bulk materials, measured with respect to the average electrostatic potential  $\bar{V}$  (that is arbitrary and may be set to zero for a bulk solid).  $\Delta E_{BS}$  is, by definition, a bulk property of the two constituent solids, and can be obtained from standard bulk band-structure calculations for SiC

and strained GaN, respectively. The spin-orbit coupling influences  $\Delta E_{BS}$  and consequently the band offsets by less than 0.01 eV in the presently studied systems. Relativistic effects have therefore been neglected.

### III. COMPUTATIONAL DETAILS

The present calculations are based on the first-principles total-energy pseudopotential method within the local-density-functional formalism (LDA).<sup>65</sup> The LDA was implemented using the Ceperley-Alder<sup>66</sup> electron-gas exchange-correlation energy, as parametrized by Perdew and Zunger.<sup>67</sup> The Kohn-Sham equations have been solved self-consistently, employing a preconditioned conjugate gradient algorithm,<sup>68</sup> and minimizing the total energy with respect to the electronic density *and* to the ionic coordinates. The electron-ion interaction was modeled by norm-conserving, fully separable ionic pseudopotentials according to the method of Troullier and Martins.<sup>69</sup>

Pseudopotential calculations for nitrides are very demanding computationally since carbon and nitrogen have no core  $p$  states and consequently possess strongly localized  $p$ -state pseudo wave functions requiring large kinetic energy cutoffs. Additionally, the  $3d$  states of Ga overlap with the N  $2p$  and even  $2s$  wave functions in the solid GaN. Indeed, it was pointed out recently that total energy calculations with frozen Ga  $3d$  states can lead to considerable errors in the cohesive properties of GaN.<sup>25</sup> Fortunately, we found that a fully dynamic treatment of the Ga  $3d$  states is unnecessary in GaN and the related compounds, as will be shown in the following section.

#### A. Choice of pseudopotentials—bulk calculations

In order to determine transferable soft Troullier-Martins-type pseudopotentials that are suitable for interface calculations, we have first determined the lattice constants, internal strain parameters and bulk moduli of bulk zinc blende and wurtzite GaN, AlN, and SiC. The pseudopotentials have been generated with neutral atomic configurations and included angular momenta up to  $\ell=2$ , with the  $\ell=1$  component acting as local potential. The semicore Ga  $3d$  electrons have been treated as part of the frozen core, but their overlap with the valence electrons is accounted for by including the nonlinear core correction<sup>70</sup> in the exchange-correlation potential and energy. In fact, we have applied this concept to all atoms in the present calculations. For the Ga, Al, and Si atoms, well established pseudopotential cutoff radii<sup>71</sup> (in units of the Bohr radius) were used:  $r_s=r_p=2.50$ ,  $r_d=2.80$  for Ga;  $r_s=r_p=2.10$ ,  $r_d=2.40$  for Al, and  $r_s=r_p=r_d=2.10$  for Si. For C and N, cutoff radii between 1.25 and 2.70 have been tested and found to change the structural parameters of GaN, AlN, and SiC very little up to  $r_{\ell}=2.00$ . Finally, we have used  $r_s^C = r_p^C = r_d^C = 1.90$ , and  $r_s^N = r_p^N = r_d^N = 2.00$ . These pseudopotentials require a kinetic energy cutoff of only 32 Ry to yield well converged cohesive properties. The values in Table I have been obtained with 63 Ry but this higher cutoff alters total energies by less than 0.1 eV/atom, and lattice constants by less than 0.005 Å. All  $\mathbf{k}$ -space integrations for the total energy were performed with 10 and 14 special  $\mathbf{k}$  points<sup>72,73</sup> for the zinc blende and wurtzite structure, respectively.

TABLE I. Calculated lattice constants  $a$  and  $c$  in Å, dimensionless hexagonal cell-internal structural parameter  $u_{wz}$  (that equals 3/8 for ideal tetrahedral coordination) and bulk modulus  $B_0$  in Mbar of wurtzite and zinc blende structure compounds. Known experimental values are given beneath the calculated values.

Compound	$a$ (Å)	$c$ (Å)	$B_0$ (Mbar)	$u_{wz}$
GaN (wurtzite)	3.182	5.171	2.01	0.3772
	3.189 <sup>a</sup>	5.185 <sup>a</sup>	1.88–2.45 <sup>b</sup>	0.377 <sup>c</sup>
GaN (zinc blende)	4.497		1.96	
	4.52 <sup>a</sup>			
AlN (zinc blende)	4.350		1.99	
	4.38 <sup>a</sup>			
SiC (zinc blende)	4.329		2.23	
	4.36 <sup>a</sup>		2.24 <sup>d</sup>	

<sup>a</sup>Reference 1.

<sup>b</sup>Reference 25.

<sup>c</sup>Reference 80.

<sup>d</sup>Reference 77.

The important outcome of these bulk calculations is that the cohesive properties of GaN can be very accurately reproduced by treating the  $3d$  electrons as rigid core states, provided the exchange-correlation energy accounts for the total electronic density rather than the valence density only. In fact, by treating the Ga  $3d$  electrons as valence states with a kinetic energy cutoff of 250 Ry, we have found the lattice constant to change by only a small amount (from 4.497 to 4.528 Å), in contrast to the pessimistic conclusions of Ref. 25.

#### B. Choice of supercells

The numbers of SiC and GaN bulk monolayers  $n$  and  $m$ , respectively, need to be sufficiently large to suppress the interaction between the two interfaces of the supercell. For interfaces with one mixed layer, the supercell contains  $n+m+2$  layers since there are two interfaces in the supercell. The total number of atoms in the unit cell depends on the lateral reconstruction. For a  $p \times q$  reconstruction, it is given by  $(n+m+2) \times p \times q$ , where the  $c(2 \times 2)$  corresponds to  $p=q=\sqrt{2}$ . Analogously, interfaces with two mixed layers lead to  $(n+m+4) \times p \times q$  atoms in the supercell.

In the present calculations, we have used  $n=m=3, 5$ , or  $7$  for interfaces with a single mixed layer and  $n=3$  and  $m=5$  for the interfaces with two mixed layers, respectively. We note that the choice  $n=7$  already exceeds the critical thickness of GaN on SiC substrate.<sup>74</sup>

Our initial atomic configuration—that we will refer to as unrelaxed—is based on (calculated) bulk lattice constants of SiC and biaxially strained GaN for all monoatomic (001) layers. For the distance between a mixed interface layer and an adjacent bulk layer, we use a layer separation that corresponds to the latter bulk material. Two mixed interface layers are separated by the arithmetic average of the SiC and strained GaN bulk layer distances. Laterally, all atoms are put on zinc blende lattice positions.

### C. Convergence tests

Starting from this configuration, we have minimized the total energy with respect to the atomic positions in the unit cell. All Hellmann-Feynman forces and the stress tensor component in the growth direction have been required to be smaller than 0.02 and 0.002 eV Å<sup>-3</sup>, respectively. Since the reconstruction of the interface decreases its symmetry, the atoms relax both laterally away from the zinc blende positions as well as along the growth direction. It turns out that the nonuniform relaxation of atoms near the interface has a dramatic effect on the interface's formation enthalpy and VBO, as will be discussed in Sec. IV, whereas a uniform stretching of the supercell length is much less important.

All  $\mathbf{k}$ -space integrations in the supercell have been performed on consistent  $\mathbf{k}$ -point meshes<sup>75</sup> that are equivalent to 10 Monkhorst-Pack<sup>72</sup> points for a bulk zinc blende structure. Denser meshes (19 points) changed the formation enthalpies by less than 0.001 eV and the VBO by less than 0.05 eV. Similarly, we have found these quantities to change by less than 0.02 eV when the number of plane waves is increased by using a kinetic energy cutoff of 100 Ry.

The convergence of  $\delta H_{\text{int}}$  with increasing interface separation  $n$  has been checked for all relaxed  $c(2 \times 2)$  interfaces by calculating superlattices with  $n, m = 3, 5, \text{ and } 7$ . The enthalpies change by less than 0.05 eV from  $n = m = 3$  to  $n = m = 7$ , in spite of the fact that  $n = 5$  supercells have a different symmetry than the others. This indicates an acceptably small interface-interface interaction. Due to the extended character of the top valence states and the high polarity of the interfaces, the calculated band offsets are, unfortunately, less well converged and depend more sensitively on  $n$ . With  $n = m = 3, 5, \text{ and } 7$ , we obtained valence-band offsets of 1.4, 1.4, and 1.8 eV for the [Si,Ga] and 0.2, 0.5, and 0.8 eV for the [C,N]  $c(2 \times 2)$  interface, respectively. Fortunately, we find at least the *differences* between the band offsets of different structures to be practically identical for  $n = 5$  and  $n = 7$ . Taking these convergence properties into account, we consistently employed supercells with  $n = m = 5$  and  $n = 5, m = 3$  for the total energy studies of GaN/SiC interfaces with one and two mixed layers, respectively. All table entries presented below for GaN/SiC interfaces have been obtained with these geometries. For the accurate prediction of the GaN/SiC and AlN/SiC band offsets as well as for the determination of the cohesive properties of the AlN/SiC interfaces, we used the maximum number of atomic layers that we were able to handle computationally, namely,  $n = m = 7$ .

## IV. RESULTS AND DISCUSSION

### A. Stability and lattice relaxation of GaN/SiC(001) interfaces

First, we have calculated the formation enthalpies of *unrelaxed* GaN/SiC(001) interfaces containing a single mixed atomic layer and a  $c(2 \times 2)$  lateral unit cell. All these formation enthalpies turn out to be positive, indicating the metastability of the underlying structures. However, the calculations reveal striking differences between the interfaces depicted symbolically in Eq. (2). The [Si,N] and [C,Ga] interfaces with C-N and Si-Ga nonsaturated bonds are highly

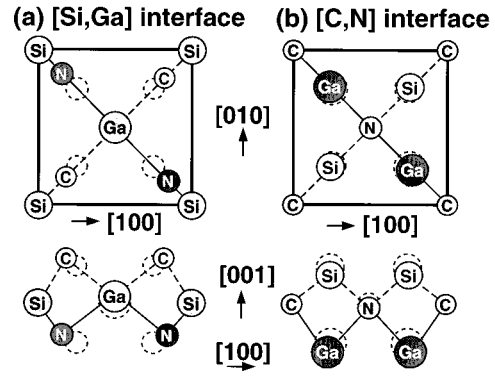


FIG. 6. Projections of the atomic positions in the mixed interface layer and the two adjacent monolayers onto a (001) (upper panel) and a (010) (lower panel) plane for a (a) [Si,Ga] type and (b) [C,N] type GaN/SiC(001) interface with  $c(2 \times 2)$  lateral reconstruction. Atoms in different (001) layers are shaded differently and dotted circles represent unrelaxed atomic positions. In order to emphasize the effects of relaxation, the distances between relaxed and unrelaxed positions have been rescaled by a factor of five.

unstable with  $\delta H_{\text{int}} = 4.47$  and 5.08 eV, in contrast to the [Si,Ga] and [C,N] interfaces with  $\delta H_{\text{int}} = 0.28$  and 0.17 eV, respectively.

These findings can easily be understood qualitatively in terms of empirical covalent radii  $r_{\text{cov}}$  and covalent bond lengths  $d_{\text{cov}}^{A-B} = r_{\text{cov}}^A + r_{\text{cov}}^B$  of nearest-neighbor atoms  $A$  and  $B$ .<sup>76</sup> Indeed, the covalent bond lengths of the “wrong bonds”  $d_{\text{cov}}^{\text{Ga-C}} = 2.03$  Å and  $d_{\text{cov}}^{\text{Si-N}} = 1.87$  Å are close to those of Si-C and Ga-N that equal 1.94 and 1.96 Å, respectively. By contrast, the bond lengths  $d_{\text{cov}}^{\text{C-N}} = 1.47$  Å and  $d_{\text{cov}}^{\text{Si-Ga}} = 2.43$  Å deviate strongly from the lengths of the Si-C and Ga-N backbonds. Consequently, the C-N and Si-Ga bonds are strongly stretched and compressed, respectively. Atomic relaxation tends to diminish these discrepancies, but cannot remove the huge misfits in bond lengths completely since any deformations of the surrounding backbonds in the interface structure cost too much energy. Accordingly, we find the interface formation enthalpies for the [Si,N] and [C,Ga] interfaces to remain large and of the order of 2 eV even after full lattice relaxation. Thus, we predict that the two latter types of interfaces do not form. The same arguments also justify *a posteriori* the exclusion of interfaces with C-C and Si-Si bonds, since  $d_{\text{cov}}^{\text{C-C}} = 1.54$  Å and  $d_{\text{cov}}^{\text{Si-Si}} = 2.34$  Å is again far away from the bulk bond lengths. We note that similar conclusions were reached in recent calculations of thin GaN films on a 6H SiC substrate.<sup>44</sup>

We now turn to the effects of lattice relaxation. Figure 6 depicts the atomic positions near the fully relaxed  $c(2 \times 2)$  [Si,Ga] and [C,N] interfaces between SiC and GaN. The relaxation changes the bond lengths between the atoms in the interface layer and the surrounding layers by as much as 0.1 Å. The predominant effect of lattice relaxation is easy to understand: the C and N atoms move towards the Si atoms and away from the bigger Ga atoms. In the case of the [Si,Ga] interface, this implies a predominantly lateral relaxation of the C and N atoms next to the interface that tends to compress the Si-N and Si-C bonds and to stretch the N-Ga and Ga-C bonds at the same time. The interface atoms (C

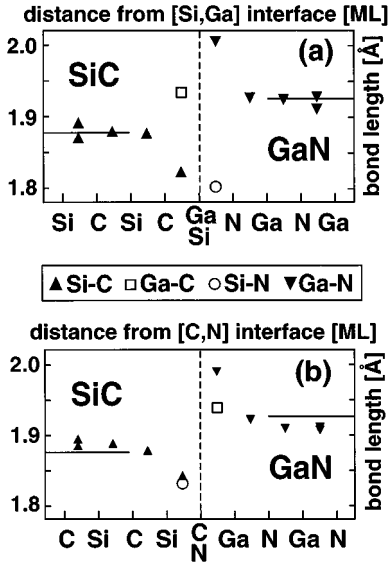


FIG. 7. Bond lengths (in Å) near the GaN/SiC(001) interface as a function of the distance from the interface. The type of mixed interface layer is (a) [Si,Ga] and (b) [C,N]  $c(2 \times 2)$ . Symmetry allows two different bond lengths between atoms belonging to certain adjacent (001) layers.

and N) in the [C,N] interface, on the other hand, relax predominantly vertically towards the neighboring Si layer and away from the opposite Ga layer. Figure 7 shows that there are also long-range distortions associated with the lattice relaxation. Even four monolayers away from the interface, the two structurally not equivalent bonds still differ by 0.02 Å from each other. Similar relaxation effects have been observed for all investigated interface structures.

Tables II and III summarize our numerical results for formation enthalpies of the physically relevant interface structures for GaN/SiC. It is evident that the atomic relaxation reduces  $\delta H_{\text{int}}$  significantly. In fact, it even alters the relative stability of various structures. Whereas the [C,N] mixed layer is energetically favored in the (unrealistic) unrelaxed configuration, the fully relaxed [Si,Ga] interface has a lower energy than the [C,N] one.

TABLE II. Calculated interface formation enthalpies  $\delta H_{\text{int}}$  (in eV) of  $c(2 \times 2)$ ,  $2 \times 1$ , and  $1 \times 2$  reconstructed and fully relaxed interface structures with a single mixed interface layer containing an equal concentration of two types of atoms specified in the first column. Values in brackets refer to unrelaxed structures. The first four rows refer to GaN/SiC(001) and the last four rows to AlN/SiC(001) interfaces, respectively.

Interface atoms	$c(2 \times 2)$	$2 \times 1$	$1 \times 2$
[Si,Ga]	0.04 (0.28)	0.14 (0.38)	0.15 (0.38)
[C,N]	0.08 (0.17)	0.16 (0.27)	0.16 (0.27)
[Si,Al]	0.34 (0.46)		
[C,N]	0.36 (0.43)		

TABLE III. Calculated formation enthalpies (in eV) and valence-band offsets (in eV) of  $2 \times 2$  reconstructed and fully relaxed GaN/SiC interfaces with two mixed monolayers. A positive band offset indicates an energetically higher valence-band maximum in SiC. Values in brackets refer to unrelaxed structures.

	$2 \times 2(4)$		$2 \times 2(5)$	
	$ca$	$ac$	$ca$	$ac$
$\delta H_{\text{int}}$	0.23 (0.36)	0.24 (0.35)	0.38 (0.53)	0.37 (0.52)
$\Delta E_V$	0.8 (0.5)	0.8 (0.6)	0.8 (0.5)	0.9 (0.6)

An important finding is the lateral  $c(2 \times 2)$  reconstruction to be systematically more stable than the  $2 \times 1$  and  $1 \times 2$  ones. This result is indicative of another important selection rule for the type of relaxed interfaces that are likely to form in real systems and may be understood in terms of the following simple electrostatic arguments, similar to those developed by Kley and Neugebauer<sup>52</sup> for the ZnSe/GaAs system. Systems that possess nonsaturated bonds are known to show a significant amount of charge transfer from the donor towards the acceptor bonds.<sup>51,52,54,60</sup> Clearly, the electrostatic energy associated with this charge transfer increases in proportion to the separation between the positively and negatively charged bonds. Consequently, a lateral reconstruction that distributes the nonsaturated bonds in a homogeneous manner across the unit cell is energetically more favorable since it leads to smaller average distances between donor and acceptor bonds.

As a simple measure of this homogeneity, one may use the ratio  $N_{wr} = (\sum_i n_i) / N_{\text{ns}}$ , where the sum runs over all  $N_{\text{ns}}$  nonsaturated bonds in the system and  $n_i$  is the number of nonsaturated bonds that are nearest neighbors of bond  $i$ . The index  $wr$  stands for “wrong bonds.” In a tetrahedral lattice, each bond possesses six nearest-neighbor bonds, so that  $N_{wr}$  cannot exceed six. In addition,  $N_{wr}$  cannot be lower than one in a charge compensated interface with a single mixed layer. For the  $c(2 \times 2)$ ,  $2 \times 1$ , and  $1 \times 2$  reconstruction patterns shown in Fig. 3, we find  $N_{wr} = 1.0, 1.5$ , and  $1.5$ , respectively. Thus, the  $c(2 \times 2)$  structure is the optimal bond arrangement from an electrostatic point of view.

These electrostatic arguments explain qualitatively the major trends in the calculated formation enthalpies of interface structures that differ only in their lateral atomic arrangement (cf. Table II). The  $c(2 \times 2)$  structures are the most stable ones, and the  $2 \times 1$  and  $1 \times 2$  patterns are energetically degenerate. Table II shows that even the formation enthalpies of the [Si,Ga] and [C,N] interfaces with  $2 \times 1$  and  $1 \times 2$  reconstructions are very close to each other, even though these structures do have different interface atoms but can be transformed into each other by swapping cations and anions and possess the same number of unsaturated bonds. In this case, electrostatic arguments still seem to be applicable.

The formation enthalpies  $\delta H_{\text{int}}$  of the reconstructed interfaces with two mixed layers, given in Table III, turn out to be systematically higher than those with one mixed layer. The  $2 \times 2(4)$  lateral reconstruction contains less nonsaturated bonds than the  $2 \times 2(5)$  pattern. Thus, the former structure is chemically more favorable. In addition, it possesses a more homogeneous distribution of the nonsaturated bonds. We

TABLE IV. Calculated valence-band offsets  $\Delta E_V$  (in eV) of  $c(2 \times 2)$ ,  $2 \times 1$ , and  $1 \times 2$  reconstructed and fully relaxed interface structures with a single mixed interface layer containing an equal concentration of two types of atoms specified in the first column. A positive sign indicates an energetically higher valence-band maximum in SiC. Values in brackets refer to unrelaxed structures. The first four rows refer to GaN/SiC(001) and the last four rows to AlN/SiC(001) interfaces, respectively.

Interface atoms	$c(2 \times 2)$	$2 \times 1$	$1 \times 2$
[Si,Ga]	1.4 (1.1)	1.4 (1.1)	1.3 (1.0)
[C,N]	0.5 (-0.4)	0.4 (-0.4)	0.4 (-0.4)
[Si,Al]	2.4 (2.4)		
[C,N]	1.5 (0.7)		

find  $N_{wr}$  to equal 1.0 for the  $2 \times 2(4)$  and 2.1 for the  $2 \times 2(5)$  structures, respectively. According to the electrostatic arguments given above, one may expect a near degeneracy of the  $ca$  and  $ac$  monolayer sequences since they differ only by a cation-anion swap (see Fig. 4), and the numerical results confirm this picture indeed.

### B. Valence-band offsets of GaN/SiC(001) interfaces

In Table IV, the calculated valence-band offsets for structures with one mixed monolayer are given. All VBO's of the relaxed structures are positive, indicating that the topmost valence state lies energetically higher in SiC than in any of the nitride compounds discussed in this paper.

In the unrelaxed superlattices, the VBO's converge rapidly with the number of bulk layers between the interfaces. For these structures, already two monolayers away from the interface the averaged potential  $\bar{V}$  reaches its asymptotic bulk value. This is similar to findings for previously studied interfaces.<sup>50,52,64</sup> With fully relaxed atomic positions, however, the plateaus in  $\bar{V}(z)$  several layers away from the interface are less flat, as depicted in Fig. 8. This is a consequence of the significant charge transfer between the donor and acceptor bonds in the interface layer that is induced by

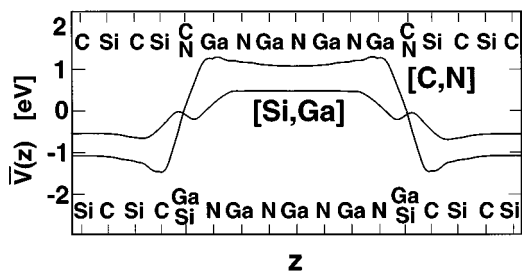


FIG. 8. Macroscopically averaged electrostatic potential  $\bar{V}(z)$  (in eV) in a supercell that models a [Si,Ga] type and [C,N] type GaN/SiC(001) interface with one mixed layer.

the large lattice relaxation. It leads to longer range contributions to  $\bar{V}(z)$ , which causes the VBO's to be more sensitive to the stoichiometric composition of the interface. Accordingly, the VBO associated with the [Si,Ga] and the [C,N] interfaces differ by as much as 1 eV, in spite of their formation enthalpy being almost the same (see Tables II and IV).

The band offsets of all  $2 \times 2$  reconstructed interfaces (Table III) with two mixed layers are, to a good approximation, degenerate and lie in the middle between the two offset groups given by the heterostructures with a single mixed atomic layer.

According to Eq. (6), the VBO can be split up into a bulk contribution that is the same for all GaN/SiC or AlN/SiC interfaces, and a term proportional to the interface dipole moment. We find the bulk term to equal 2.93 and 3.32 eV for GaN/SiC and AlN/SiC, respectively. Thus, the charge redistribution at the polar interfaces reduces this contribution by more than a factor of two.

### C. Stability and valence-band offsets of AlN/SiC(001) interfaces

Tables II and IV also contain the results of formation enthalpies and band offsets for  $c(2 \times 2)$  reconstructed AlN/SiC interfaces. Compared to GaN/SiC, the lattice mismatch is considerably smaller and amounts to only  $\approx 0.5\%$ . In addition, the ‘‘chemical’’ mismatch between the atoms in the interface (Si-Al versus Si-Ga) is less pronounced. Consequently, the relaxed bond lengths at the interface are much closer to each other than in the GaN/SiC case. For example, we obtain 1.83, 1.93, 1.85, and 1.92 Å for the Si-C, Al-N, Si-N, and Al-C bonds, respectively, at the [C,N]  $c(2 \times 2)$  interface.

Remarkably, we find the formation enthalpies of the AlN/SiC interfaces to be about five times *higher* than those of the corresponding GaN/SiC interfaces. The reason lies in the relative stability of the zinc blende and wurtzite phases of AlN and GaN. Whereas the hexagonal bulk phase of GaN is only slightly more stable than the cubic phase, we find the total energy difference between these phases to be more than twice as large in AlN, namely, 28.9 meV/atom compared to 10.2 meV/atom in GaN. Thus, the pseudomorphic growth of AlN on a cubic substrate is energetically less favorable, in spite of the lower strain.

The chemical trends in the VBO's of AlN/SiC heterostructures are similar to those in the GaN/SiC system. In particular, the VBO of the [C,N] interface is smaller than that of the [Si,Al] interface whereas the formation enthalpies are almost identical. All band offsets calculated in this paper, including the discontinuities in the conduction bands, are summarized in Fig. 9. The nitride energy gaps represent computed *GW*-corrected LDA energy gaps,<sup>29</sup> and the SiC gap equals the experimental value.<sup>77</sup> Since the precise VBO values depend on the detailed type and structure of the interface, these heterostructures can only be characterized by a range of VBO's rather than by a single number. This is indicated by the shaded energy ranges in the figure. In spite of these uncertainties, the present calculations predict that the AlN/SiC(001) and GaN/SiC(001) heterostructures are of type I and II, respectively.

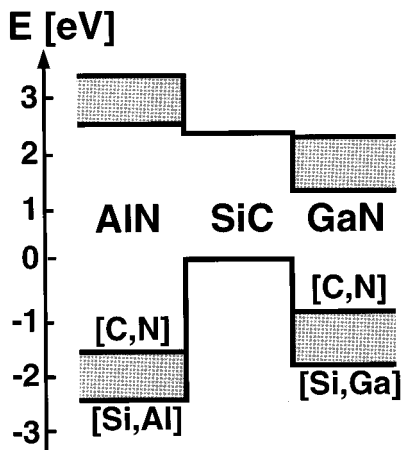


FIG. 9. Predicted band offsets between [001]-oriented, cubic SiC substrate and pseudomorphic epitaxial GaN and AlN. Note that the fundamental band gap of zinc blende AlN is indirect (from  $\Gamma$  to X).

#### D. Comparison with experiment

To the best of our knowledge, no direct experimental measurements of the band offsets in cubic GaN/SiC(001) and AlN/SiC(001) heterostructures have been performed up to now. Based on measurements of Schottky barrier heights and AlN/GaN wurtzite band offsets, Wang *et al.*<sup>78</sup> estimated a VBO of 1.2 eV for GaN/SiC and of 1.85 eV for AlN/SiC. These values seem to agree with our predictions, although the data disregarded any interface orientation effects. The VBO of 0.8 eV between wurtzite AlN and 6H SiC given by Benjamin *et al.*<sup>79</sup> is not too far from our values either.

The strong dependence of the VBO on the structural details of the GaN/SiC and AlN/SiC interfaces suggests that the VBO's in these systems may be dependent on the crystal growth conditions and vary significantly over a macroscopic sample. These variations reflect local changes in the interface

dipole moment that accounts for a significant portion of the total VBO, as discussed above. Such a clear relation between VBO's and growth conditions has been recently observed experimentally for polar ZnSe/GaAs(001), ZnSe/Ge(001), and Ge/GaAs(001) heterostructures.<sup>47,48</sup>

#### V. CONCLUSIONS

We have presented *ab initio* studies of the stability of various reconstructed polar GaN/SiC(001) and AlN/SiC(001) interface geometries with one and two mixed layers at the interface. The preferred bonding configurations at the interfaces have been found to be Si-N and Ga-C (Al-C). Our calculations indicate that the interfaces with a single mixed layer and with a  $c(2 \times 2)$  lateral arrangement are the most stable ones. The relative enthalpies of structures that differ only in their lateral atomic arrangements can be understood qualitatively by simple electrostatic arguments. Our results indicate the atomic relaxation at the GaN/SiC(001) and AlN/SiC(001) interfaces to play a crucial role in determining formation enthalpies and band discontinuities. Our self-consistent total-energy minimizations show that the magnitude and direction of the atomic relaxations are qualitatively in accord with the different covalent radii of the constituent atoms and steric arguments.

The calculated VBO's depend strongly on the interface dipole moment that reflects the chemical composition of the interface, but are less sensitive to the type of lateral reconstruction. The GaN/SiC(001) and AlN/SiC(001) heterostructures are predicted to be of type II and I, respectively, with the absolute valence-band maximum lying in SiC. The calculated VBO's lie in the range from 0.8 to 1.8 eV for GaN/SiC, and between 1.5 and 2.4 eV for AlN/SiC.

#### ACKNOWLEDGMENTS

This work was supported by the Deutsche Forschungsgemeinschaft and the Bayerische Forschungverbund FOROPTO.

<sup>1</sup>S. Strite, M. E. Lin, and H. Morkoç, *Thin Solid Films* **231**, 197 (1993).  
<sup>2</sup>H. Morkoç, S. Strite, G. B. Gao, M. E. Lin, B. Sverdlov, and M. Burns, *J. Appl. Phys.* **76**, 1363 (1994), and references therein.  
<sup>3</sup>M. Asif Khan, J. N. Kuznia, A. R. Bhattarai, and D. T. Olson, *Appl. Phys. Lett.* **62**, 1786 (1993).  
<sup>4</sup>S. Nakamura, *Jpn. J. Appl. Phys., Part 2* **35**, L74 (1996).  
<sup>5</sup>M. Asif Khan, J. N. Kuznia, D. T. Olson, T. George, and W. T. Pike, *Appl. Phys. Lett.* **63**, 3470 (1993).  
<sup>6</sup>Z. Sitar, M. J. Paisley, B. Yan, J. Ruan, J. W. Choyke, and R. F. Davis, *J. Vac. Sci. Technol. B* **8**, 316 (1990).  
<sup>7</sup>S. Yoshida, S. Misawa, and S. Gonda, *J. Vac. Sci. Technol. B* **1**, 250 (1983).  
<sup>8</sup>F. A. Ponce, J. S. Major, Jr., W. E. Plano, and D. F. Welch, *Appl. Phys. Lett.* **65**, 2302 (1994).  
<sup>9</sup>A. Salvador, G. Liu, W. Kim, O. Aktas, A. Botchkarev, and H. Morkoç, *Appl. Phys. Lett.* **67**, 3322 (1995).  
<sup>10</sup>S. Strite and H. Morkoç, *J. Vac. Sci. Technol. B* **10**, 1237 (1992).  
<sup>11</sup>R. F. Davis, *Physica B* **185**, 1 (1993).

<sup>12</sup>J. G. Kim, A. C. Frenkel, H. Liu, and R. M. Park, *Appl. Phys. Lett.* **65**, 91 (1994).  
<sup>13</sup>J. Paisley, Z. Sitar, J. B. Posthill, and R. F. Davis, *J. Vac. Sci. Technol. A* **7**, 701 (1989).  
<sup>14</sup>H. Liu, C. Frenkel, J. G. Kim, and R. M. Park, *J. Appl. Phys.* **74**, 6124 (1993).  
<sup>15</sup>H. Okumura, S. Yoshida, and T. Okahisa, *Appl. Phys. Lett.* **64**, 2997 (1994).  
<sup>16</sup>A. Barski, U. Rössner, J. L. Rouviere, and M. Arley, *MRS Internet J. Nitride Semicond. Res.* **1**, 21 (1996).  
<sup>17</sup>R. L. Headrick, S. Kycia, Y. K. Park, A. R. Woll, and J. D. Brock, *Phys. Rev. B* **54**, 14 686 (1996).  
<sup>18</sup>I. Petrov, E. Mojab, R. C. Powell, J. E. Greene, L. Hultman, and J.-E. Sundgren, *Appl. Phys. Lett.* **60**, 2491 (1992).  
<sup>19</sup>S. Tanaka, R. S. Kern, and R. F. Davis, *Appl. Phys. Lett.* **66**, 37 (1995).  
<sup>20</sup>J. Chaudhuri, R. Thokala, J. H. Edgar, and B. S. Sywe, *J. Appl. Phys.* **77**, 6263 (1995).  
<sup>21</sup>T. Sasaki and T. Matsuoka, *J. Appl. Phys.* **64**, 4531 (1988).

- <sup>22</sup>C. Wetzel, D. Volm, B. K. Meyer, K. Pressel, S. Nilsson, E. N. Mokhov, and P. G. Baranow, *Appl. Phys. Lett.* **65**, 1033 (1994).
- <sup>23</sup>W. A. Harrison, E. A. Kraut, J. R. Waldrop, and R. W. Grant, *Phys. Rev. B* **18**, 4402 (1978).
- <sup>24</sup>R. M. Martin, *J. Vac. Sci. Technol. B* **17**, 978 (1980).
- <sup>25</sup>A. F. Wright and J. S. Nelson, *Phys. Rev. B* **50**, 2159 (1994); see there the references to older papers.
- <sup>26</sup>J. A. Majewski, M. Städele, and P. Vogl, *MRS Internet J. Nitride Semicond. Res.* **1**, 30 (1996).
- <sup>27</sup>N. E. Christensen and I. Gorczyca, *Phys. Rev. B* **50**, 4397 (1994).
- <sup>28</sup>K. Kim, W. R. L. Lambrecht, and B. Segall, *Phys. Rev. B* **50**, 1502 (1994).
- <sup>29</sup>A. Rubio, J. L. Corkill, M. L. Cohen, E. L. Shirley, and S. G. Louie, *Phys. Rev. B* **48**, 11 810 (1993).
- <sup>30</sup>M. Palummo, L. Reining, R. W. Godby, C. M. Bertoni, and N. Börnsen, *Europhys. Lett.* **26**, 607 (1994).
- <sup>31</sup>W. R. L. Lambrecht, B. Segall, J. Rife, W. R. Hunter, and D. K. Wickenden, *Phys. Rev. B* **51**, 13 516 (1995).
- <sup>32</sup>E. A. Albanesi, W. R. L. Lambrecht, and B. Segall, *Phys. Rev. B* **48**, 17 841 (1993).
- <sup>33</sup>P. E. Van Camp, V. E. Van Doren, and J. T. Devreese, *Phys. Rev. B* **44**, 9056 (1994).
- <sup>34</sup>M. Suzuki, T. Uenoyama, and A. Yanase, *Phys. Rev. B* **52**, 8132 (1995).
- <sup>35</sup>K. Kim, W. R. L. Lambrecht, and B. Segall, *Phys. Rev. B* **53**, 16 310 (1996).
- <sup>36</sup>Su-Huai Wei and Alex Zunger, *Appl. Phys. Lett.* **69**, 2719 (1996).
- <sup>37</sup>A. Rubio, J. L. Corkill, and M. L. Cohen, *Phys. Rev. B* **49**, 1952 (1994).
- <sup>38</sup>S.-H. Ke, M.-C. Huang, and R.-Z. Wang, *Solid State Commun.* **89**, 105 (1994).
- <sup>39</sup>E. A. Albanesi, W. R. L. Lambrecht, and B. Segall, *J. Vac. Sci. Technol. B* **12**, 2470 (1994).
- <sup>40</sup>K. Nath and A. B. Anderson, *Phys. Rev. B* **40**, 7916 (1989).
- <sup>41</sup>S. Y. Ren and J. D. Dow, *Appl. Phys. Lett.* **69**, 251 (1996).
- <sup>42</sup>L. K. Teles, L. M. R. Scolfaro, R. Enderlein, J. R. Leite, A. Josiek, D. Schikora, and K. Lischka, *J. Appl. Phys.* **80**, 6322 (1996).
- <sup>43</sup>W. R. L. Lambrecht and B. Segall, *Phys. Rev. B* **43**, 7070 (1991).
- <sup>44</sup>R. B. Capaz, H. Lim, and J. D. Joannopoulos, *Phys. Rev. B* **51**, 17 755 (1995).
- <sup>45</sup>R. Di Felice, J. E. Northrup, and J. Neugebauer, *Phys. Rev. B* **54**, R17 351 (1996).
- <sup>46</sup>K. Kunc and R. M. Martin, *Phys. Rev. B* **24**, 3445 (1981).
- <sup>47</sup>G. Bratina, L. Vanzetti, L. Sorba, G. Biasiol, A. Franciosi, M. Peressi, and S. Baroni, *Phys. Rev. B* **50**, 11 723 (1994).
- <sup>48</sup>R. Nicolini, L. Vanzetti, G. Mula, G. Bratina, L. Sorba, A. Franciosi, M. Peressi, S. Baroni, R. Resta, A. Baldereschi, J. E. Angelo, and W. W. Gerberich, *Phys. Rev. Lett.* **72**, 294 (1994).
- <sup>49</sup>D. M. Bylander and L. Kleinman, *Phys. Rev. B* **41**, 3509 (1990).
- <sup>50</sup>S. Baroni, R. Resta, A. Baldereschi, and M. Peressi, in *Spectroscopy of Semiconductor Microstructures*, edited by G. Fasol, A. Fasolino, and P. Lugli (Plenum, London, 1989).
- <sup>51</sup>R. G. Dandrea, S. Froyen, and A. Zunger, *Phys. Rev. B* **42**, 3213 (1990).
- <sup>52</sup>A. Kley and J. Neugebauer, *Phys. Rev. B* **50**, 8616 (1994).
- <sup>53</sup>M. Peressi, L. Colombo, R. Resta, S. Baroni, and A. Baldereschi, *Phys. Rev. B* **48**, 12 047 (1993).
- <sup>54</sup>W. R. L. Lambrecht, C. Amador, and B. Segall, *Phys. Rev. Lett.* **68**, 1363 (1992).
- <sup>55</sup>F. A. Ponce, M. A. O'Keefe, and E. C. Nelson, *Philos. Mag. A* **74**, 777 (1996).
- <sup>56</sup>F. A. Ponce, B. S. Krusor, J. S. Major, Jr., W. E. Plano, and D. F. Welch, *Appl. Phys. Lett.* **67**, 410 (1995).
- <sup>57</sup>F. A. Ponce, C. G. Van de Walle, and J. E. Northrup, *Phys. Rev. B* **53**, 7473 (1996).
- <sup>58</sup>W. C. Hughes, W. H. Rowland, Jr., M. A. L. Johnson, S. Fujita, J. W. Cook, Jr., J. F. Schetzina, J. Ren, and J. A. Edmond, *J. Vac. Sci. Technol. B* **13**, 1571 (1995).
- <sup>59</sup>O. Brandt, H. Yang, B. Jenichen, Y. Suzuki, L. Däweritz, and K. H. Ploog, *Phys. Rev. B* **52**, 2253 (1995), and references therein.
- <sup>60</sup>W. R. L. Lambrecht and B. Segall, *Phys. Rev. B* **47**, 9289 (1993).
- <sup>61</sup>H. Holloway and L. C. Davis, *Phys. Rev. Lett.* **53**, 830 (1984).
- <sup>62</sup>T. Fuyuki, T. Yoshinobu, and H. Matsunami, *Thin Solid Films* **225**, 225 (1993); S. Hara, T. Meguro, Y. Aoyagi, M. Kawai, S. Misawa, E. Sakuma, and S. Yoshida, *ibid.* **225**, 240 (1993).
- <sup>63</sup>X.-S. Wang, K. Self, V. Bressler-Hill, R. Maboudian, and W. H. Weinberg, *Phys. Rev. B* **49**, 4775 (1994).
- <sup>64</sup>L. Colombo, R. Resta, and S. Baroni, *Phys. Rev. B* **44**, 5572 (1991).
- <sup>65</sup>W. Pickett, *Comput. Phys. Rep.* **9**, 115 (1988).
- <sup>66</sup>D. M. Ceperley and B. J. Alder, *Phys. Rev. Lett.* **45**, 566 (1980).
- <sup>67</sup>J. P. Perdew and A. Zunger, *Phys. Rev. B* **23**, 5048 (1981).
- <sup>68</sup>M. C. Payne, M. P. Teter, D. C. Allan, T. A. Arias, and J. D. Joannopoulos, *Rev. Mod. Phys.* **64**, 1045 (1992).
- <sup>69</sup>N. Troullier and J. L. Martins, *Phys. Rev. B* **43**, 1993 (1991); L. Kleinman and D. M. Bylander, *Phys. Rev. Lett.* **48**, 1425 (1982).
- <sup>70</sup>S. G. Louie, S. Froyen, and M. L. Cohen, *Phys. Rev. B* **26**, 1738 (1982).
- <sup>71</sup>J. A. Majewski, in *Proceedings of the 22nd International Conference on the Physics of Semiconductors*, edited by D. J. Lockwood (World Scientific, Singapore, 1995), p. 711.
- <sup>72</sup>H. J. Monkhorst and J. D. Pack, *Phys. Rev. B* **13**, 5188 (1976).
- <sup>73</sup>P. J. H. Denteneer and W. Van Haeringen, *Solid State Commun.* **59**, 829 (1986).
- <sup>74</sup>M. E. Sherwin and T. J. Drummond, *J. Appl. Phys.* **69**, 8423 (1991).
- <sup>75</sup>S. Froyen, *Phys. Rev. B* **39**, 3168 (1989).
- <sup>76</sup>J. Philips, *Bonds and Bands in Semiconductors* (Academic, New York, 1973).
- <sup>77</sup>*Semiconductors. Physics of Group IV Elements and III-V Compounds*, edited by O. Madelung, Landolt-Börnstein, New Series, Group III, Vol. 17, Pt. a (Springer, Berlin, 1982).
- <sup>78</sup>M. W. Wang, J. O. McCaldin, J. F. Swenberg, T. C. McGill, and R. J. Hauenstein, *Appl. Phys. Lett.* **66**, 1974 (1995).
- <sup>79</sup>M. C. Benjamin, C. Wang, R. F. Davis, and R. J. Nemanich, *Appl. Phys. Lett.* **64**, 3288 (1994).
- <sup>80</sup>H. Schulz and K. H. Thiemann, *Solid State Commun.* **23**, 815 (1977).